



PERGAMON



Atmospheric Environment ■ (■■■■) ■■■-■■■

ATMOSPHERIC
ENVIRONMENT

www.elsevier.com/locate/atmosenv

The concentrations and fluxes of total gaseous mercury in a western coastal area of Korea during the late March period of 2001

Ki-Hyun Kim Kim^{a,*}, Min-Young Kim^b, Joon Kim^c, Gangwoong Lee^d^aDepartment of Earth Sciences, Sejong Institution, Sejong University, Kun Ja Dong, Kwang Jin Goo, Seoul 143-747, South Korea^bSeoul Metropolitan Research Institute of Public Health and Environment, South Korea^cDepartment of Atmospheric Sciences, Yonsei University, South Korea^dDepartment of Environmental Sciences, Hankuk University of Foreign Studies, South Korea

Received 31 October 2001; received in revised form 9 April 2002; accepted 19 April 2002

Abstract

Factors affecting the distribution and exchange of total gaseous mercury (Hg) were investigated over a bare paddy field at Hari, a relatively clean district at Kang Hwa Island, Korea in late March 2001. The Hg concentrations were quantified at two heights (1 and 5 m above the ground), and then combined with micrometeorological measurements of turbulent exchange coefficients for flux computation. During the 8-day period of measurements, mean concentrations of Hg at 1 m ($\sim 3.89 \text{ ng m}^{-3}$) were lower than those reported from urbanized/industrialized areas but higher than the background concentration (i.e., $1\text{--}2 \text{ ng m}^{-3}$). The Hg fluxes, however, were comparable to those reported in the literature for polluted environments and showed clear diurnal pattern with maximum ($\sim 600 \text{ ng m}^{-2} \text{ h}^{-1}$) during midday and the minimum ($\sim 100 \text{ ng m}^{-2} \text{ h}^{-1}$) at nighttime. Occasionally, at nighttime when the turbulent mixing was weak under stable conditions, a deposition of Hg was observed at much lower rates (about $-32.3 \text{ ng m}^{-2} \text{ h}^{-1}$). The rate of Hg emission tended to increase with increasing air/soil temperatures and pollutant levels under enhanced turbulent mixing. By contrast, dry deposition of Hg seemed to be related to the increase of certain pollutants such as fine particles (PM 2.5) and CO. Overall, the bare paddy field was a strong source of Hg with the daily net Hg emission of $4.4 \mu\text{g m}^{-2}$ during the measurement period. © 2002 Published by Elsevier Science Ltd.

Keywords: Total gaseous mercury; Flux; Mobilization; Distribution; Background; Source; Asian dust

1. Introduction

The presence of vapor-phase elemental mercury (Hg^0) has been of special interest in the studies of air–soil exchange processes, because of its unique physicochemical properties as being predominantly vapor-phase, but metallic, constituent (Lin and Penkonen, 1999). In recent years, investigation of its exchange rates across soil–air boundary has been enhanced by the advancement of measurement techniques: (a) the development of

sensitive analytical tools to quantify minute concentration differences of Hg at multiple heights and (b) the application of eddy covariance technique to concurrently estimate turbulent transfer coefficients of Hg across those heights (e.g., Kim and Lindberg, 1994; Meyers et al., 1996; Lee et al., 2000; Edwards et al., 2001). Subsequently, several studies have been conducted under diverse settings that reflect the behavior of Hg in the clean background environments such as forest soils (Kim et al., 1995, 1997), canopies (Lindberg et al., 1998), and water bodies (Poissant and Casimir, 1998). Some of those studies were further extended to the complicated environmental settings that are under the

*Corresponding author. Tel.: +822-3408-3233; fax: +822-499-2354.

E-mail address: khkim@sejong.ac.kr (K.-H. Kim Kim).

1 influences of excessive source processes with the natural
 3 (Gustin et al., 1996) and/or anthropogenic origin
 5 (Lindberg et al., 1995; Wallschlager et al., 2000; Kim
 7 et al., 2001).

5 To comply with the growing demand of extending the
 7 Hg database, we have attempted to develop a confident
 9 method that will allow us to derive reliable flux of Hg in
 11 the fast urbanizing areas in the far East Asia (e.g., Kim
 13 and Kim, 1999). With an aim of demonstrating the
 15 capability of our approach, we conducted the micro-
 17 meteorological measurements of Hg fluxes from a
 19 gigantic landfill area in the metropolitan city of Seoul
 21 in 2000 (Kim et al., 2001). As a succession of our efforts
 23 to acquire a better knowledge on Hg geochemistry, the
 25 present study was undertaken to measure Hg fluxes from
 27 a relatively clean site in a western coast of Korean
 peninsula in late March 2001. The 8-day period of our
 study (20–27 March 2001) coincided with the intensive
 Asian Dust (hereafter referred to as AD) period. Hence,
 both distribution and mobilization characteristics of Hg
 during this study period might have been influenced by
 intense AD events to some extent. In the present study
 based on our flux measurements made at Kang Hwa
 Island, we provide some insights into the effects of
 various processes on Hg exchange over an area under
 the combined influence of both natural and anthropo-
 genic sources.

31 2. Materials and methods

33 2.1. Site characteristics and environmental conditions of 35 the study period

37 The site of our selection, Kang Hwa Island is located
 39 on the western coastal area of Korea (latitude: 37°43'N;
 41 longitude: 126°18'E). The site was located in a rice
 43 paddy of Hari district, Kang Hwa Island in Korea
 45 (Figs. 1 and 2). The surface soil was dry because the field
 47 had not been irrigated for more than 5 months after
 49 harvest in mid-October. During the study, all the
 51 relevant meteorological and environmental parameters
 53 were measured concurrently with an automated moni-
 55 toring system in a mobile van, along with three
 micrometeorological towers. The results of those mea-
 surements are summarized in Tables 1 and 2. During
 this study, the prevailing wind direction was either NW
 (daytime) or N (nighttime). The wind speeds were
 gradually rising throughout the study period with the
 mean of $3.6 + 3.0 \text{ m s}^{-1}$ (range: $0.1\text{--}11.2 \text{ m s}^{-1}$, $N = 168$).
 Because of the AD, the concentrations of particulate
 matters were unusually high. The PM concentrations,
 measured in terms of PM 2.5 and PM 10, averaged 132
 (+87) and 274 (+233) $\mu\text{g m}^{-3}$, respectively.

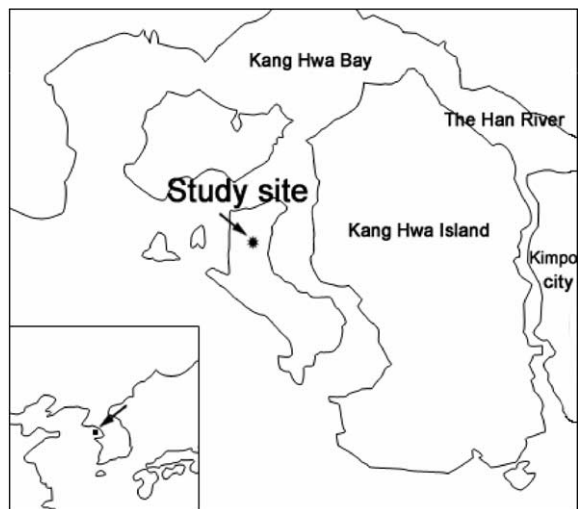


Fig. 1. A map depicting geographical location of the study site. Kang Hwa Island is located on the western coastal area of Korea.

2.2. Micrometeorological measurement

It is essential to know turbulent transfer coefficients (K) for the computation of trace gas fluxes, once its concentration gradients are quantified between the two measurement heights. It is generally assumed that the mechanism regulating the turbulent transport is indiscriminant among scalar quantities. Hence, the fluxes of Hg can be estimated indirectly, if K values for other scalar (such as heat or water vapor) are derived. During our study, eddy covariance measurements were made on three independent towers (placed about 20 m apart each other). Each tower was equipped with a tri-axial sonic anemometer at 3 m above ground. The flux measurements made at 3 m above the ground would require a minimum fetch of 300 m for prevailing wind directions. The study site was a flat, homogeneous paddy field with sufficient fetches of 2–3 km for all wind directions. The concentration gradient of Hg was measured next to the 3 m tower located in the middle. Unfortunately, the flux data from this middle tower were not produced due to breakage of its data-logger. However, one of the remaining towers was 10 m high and the flux measurements of sensible heat and momentum were made at four heights (i.e., 1, 3, 6.4, and 9 m). Using these measurement data, we have computed the turbulent exchange coefficient for mercury, K_{Hg} based on Reynolds analogy (i.e., $K_m = K_h = K_{\text{Hg}}$, where subscripts m, h, and Hg represent momentum, heat, and mercury, respectively). The effects of atmospheric stability on these relationships can be taken into account as follows:

$$K_h/K_m \approx K_{\text{Hg}}/K_m = \phi_m/\phi_h,$$

where ϕ_m and ϕ_h are the non-dimensional forms for

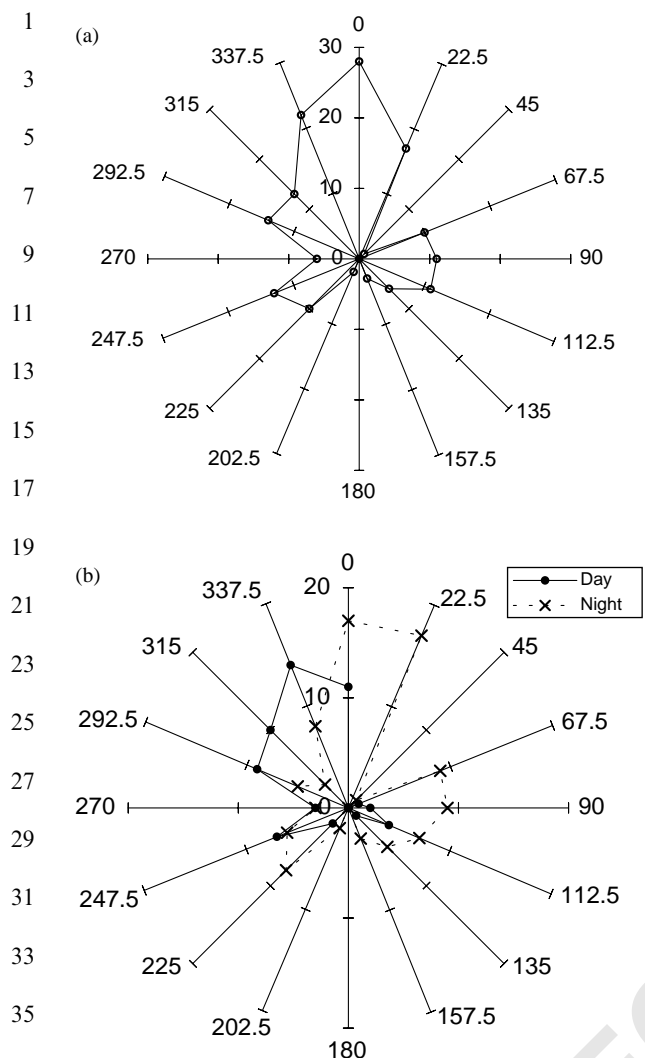


Fig. 2. A plot of windrose pattern for the study area using (a) all and (b) diurnally divided data sets. The total number of wind occurrences for each of 16 directions are compared.

wind shear and thermal stratification, respectively; they can be described as a function of the Monin–Obukhov stability parameter (z/L) such as

$$\phi_m = \begin{cases} (1 + 16|z/L|)^{-1/4}, & -2 \leq z/L \leq 0, \\ (1 + 5z/L), & 0 \leq z/L \leq 1, \end{cases}$$

$$\phi_h = \begin{cases} (1 + 16|z/L|)^{-1/2}, & -2 \leq z/L \leq 0, \\ (1 + 5z/L), & 0 \leq z/L \leq 1. \end{cases}$$

In a neutrally stratified conditions, we can represent K_m with the dimension of length \times velocity. It then holds the following relationship with reference height z_r and friction velocity u^* (Kaimal and Finnigan, 1994):

$$K_m = ku^* z_r,$$

where k is known as the von Karman constant. It is obvious that the term, K_m is proportional to the measurement height. Hence, the final equation for K_{Hg} can be written as

$$K_{Hg} = ku^* z_r * (\phi_m / \phi_h).$$

Since the concentrations were measured at $z_1 = 1$ and $z_2 = 5$ m, the geometric mean of these values, that is, $(z_1 z_2)^{1/2} \approx 2.236$ m was used as the reference height z_r . The values of u^* and z/L were obtained directly from the sonic anemometer at 3 m above ground. We have checked the constancy of u^* and z/L for the first 10 m surface layer and found the variations to be $< 10\%$. Values of the exchange coefficients (i.e., K_h , K_m) from the two different towers also agreed for the same measurement height of 3 m on average within 5% during daytime, suggesting the reasonable homogeneity and flatness of the site. In the final computation of K_{Hg} , we used the values averaged from the two 3 m tower measurements.

2.3. Air sampling and analysis

The measurements of total gaseous Hg and relevant parameters were made concurrently from 20 to 27 March 2001. The procedures for sampling and analysis of vapor-phase Hg have been described in detail in Kim et al. (2001). In this study, the atmospheric Hg concentrations were measured hourly at 1 and 5 m above the ground. A total of 164 hourly data were collected from both levels using two individual on-line automatic Hg measurement systems (AM-2 model, the Nippon Instrument Co., Japan) with the internally combined sampling/detection devices. For each hourly interval, total gaseous Hg was collected by an Au-amalgam trap at a constant but moderate flow rate of 11 min^{-1} , desorbed thermally, and detected at wavelength of 253.7 nm by a non-dispersive double beam, flameless atomic absorption system. The system exhibited absolute detection limit of ca 1 pg of Hg. The precision of individual analytical systems, if evaluated in terms of relative standard error ($\text{RSE} = \text{mean} \times 100/\text{SE}$) of five replicate injection data of vapor-phase standards, was generally found at 0.5% level. The accuracy of the analytical system cannot be assessed directly owing to the unavailability of certified vapor standards. However, when calibrated against the NBS standards (e.g., NBS-1632a, 1568, and 1575), the system yielded mean accuracy in 3–5% range. The overall precision of combined sampling plus analytical system for airborne Hg measurements was excellent in all bias tests (Kim and Kim, 1999).

Because the concentration gradient of Hg was determined as difference in its concentrations across relatively short distance, its measurement uncertainty needs to be assessed to validate the gradient computa-

Table 1
A statistical summary of Hg and relevant environmental parameters determined concurrently at hourly intervals from Hari district of Kang Hwa Island during the study period

	Hg(L) ^a (ng m ⁻³)	Hg(U) (ng m ⁻³)									
(A) Hg concentrations											
Mean	3.72	3.26									
Median	3.40	3.12									
SD	1.10	0.93									
Min	2.21	1.82									
Max	8.35	7.72									
N	164	166									
(B) Meteorological parameters											
UV (μs cm ⁻²)	RH (%)	WS (m s ⁻¹)	Temp. (°C)								
0.04	46.0	3.57	6.50								
0.00	44.0	2.95	6.35								
0.06	19.0	2.54	4.15								
0.00	18.0	0.10	-1.60								
0.23	94.0	11.2	16.5								
168	168	168	168								
(C) Relevant pollutants determined concurrently with Hg measurements											
	SO ₂ (ppb)	NO (ppb)	NO ₂ (ppb)	NO _x (ppb)	CH ₄ (ppm)	NMHC (ppm)	THC (ppm)	O ₃ (ppb)	CO (ppm)	PM2.5 (μg m ⁻³)	PM10 (μg m ⁻³)
Mean	2.55	2.18	7.34	9.51	1.67	0.49	2.14	40.9	1.66	132	274
Median	2.00	1.00	5.00	6.00	1.65	0.38	1.99	41.0	0.30	110	217
SD	2.33	2.36	7.71	9.65	0.08	0.34	0.38	12.4	3.48	87.4	233
Min	1.00	1.00	1.00	2.00	1.44	0.09	1.61	18.0	0.00	34.0	42.0
Max	14.0	15.0	47.0	62.0	2.25	1.96	3.57	74.0	21.2	476	1244
N	164	164	164	164	165	165	165	167	167	164	164
^a Capital letters L and U denote lower (1 m) and upper (5 m) height of concentration gradient measurements.											
Table 2											
A statistical summary of Hg concentrations and related parameters for the quantification of fluxes											
	Hg(L) (ng m ⁻³)	Hg(U) (ng m ⁻³)	ΔHg (ng m ⁻³)	K (m s ⁻¹)	Flux (ng m ⁻² h ⁻¹)						
(A) Upward emission events											
Mean	3.89	3.22	0.67	0.078	229						
Median	3.58	3.02	0.60	0.075	135						
SD	1.15	0.97	0.43	0.049	236						
Min	2.21	1.82	0.03	0.004	5.96						
Max	8.35	7.72	2.14	0.168	1071						
N	129	129	129	83	83						
(B) Downward dry deposition events											
Mean	3.07	3.45	-0.38	0.028	-32.3						
Median	3.05	3.23	-0.28	0.019	-18.3						
SD	0.57	0.82	0.37	0.024	37.5						
Min	2.39	2.49	-1.82	0.004	-136						
Max	5.02	6.84	-0.03	0.101	-0.387						
N	31	31	31	17	17						

tion. We employed the concept of the percent gradient (PG) (e.g., Kim and Kim, 1999):

$$\text{Percent gradient (PG)} = \frac{|\Delta C_{\text{Hgo}}|}{C_{\text{Hgo}}(\text{lower height of 1 m})} \times 100.$$

Four cases out of the total of 164 measurements were not assigned with any vertical direction (either upward or downward) because of identical concentration values between the two heights. The PG values for the remainders, when grouped into emission and dry deposition events, were averaged to be $16.6 \pm 8.9\%$ (range: 0.74–43.7%, $N = 129$) and $12.0 \pm 9.6\%$ (range: 0.79–36.3%, $N = 31$), respectively. Instrument biases of the two analyzers were checked on a regular basis and always within 1% of the measured concentrations, comparable to the mean analytical precision of the measurement system (e.g., 1%). Then the uncertainty of gradient data is unlikely to exceed 2%, because gradients are determined as concentration differences between the two heights. Based on the PG criterion of 2%, >94% of our gradient data (151 out of 160) turned out to be statistically significant.

3. Results and discussion

3.1. The environmental conditions and the overall pictures of Hg measurements

The meteorological data summarized in Table 1 reflect dynamic weather situation in the early spring of Korea. Both temperature and relative humidity (RH) exhibited moderately low values, whereas winds varied significantly with the mean of $3.6 (\pm 3.0) \text{ m s}^{-1}$. Interestingly, during this winter–spring season, the AD events had occurred with an unusually high frequency and strength. The first AD was observed as early as in January, and then reappeared more frequently later (i.e., 11 times in March, seven times in April, and three times in May). The AD events coincided with $\approx 60\%$ of our measurement period between 20 and 27 March 2001. During this study period, the first AD was observed for the limited time period on 20 March. It then resumed on 21 March and continued until 25 March. The supplementary analysis of the back-trajectory data on a daily basis indicated that the inflow of air was passing through the Gobi desert, before they reached Kang Hwa Island during most of the study period. The Gobi desert is well known for one of the major source areas for a long-range transport of aerosols in East Asia (Perry et al., 1999).

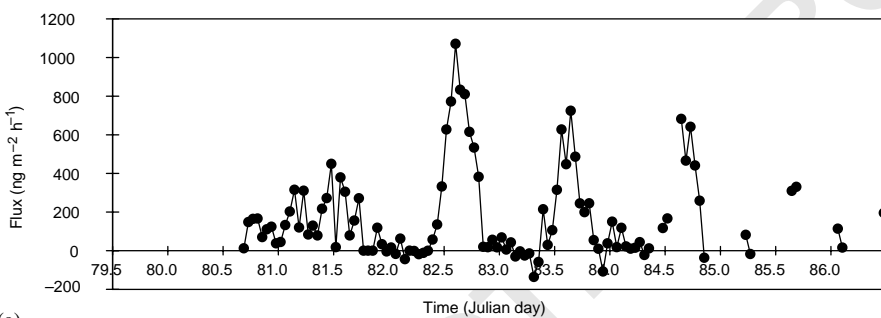
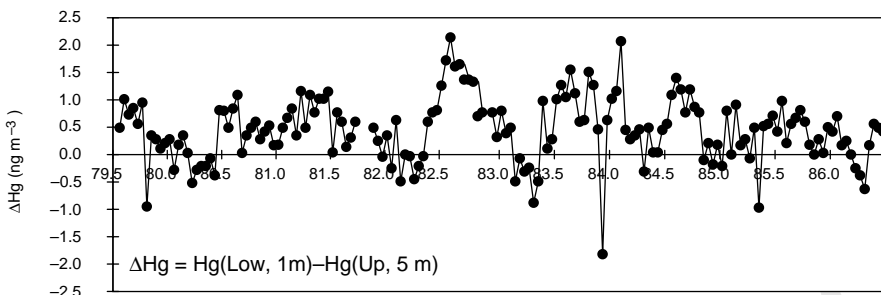
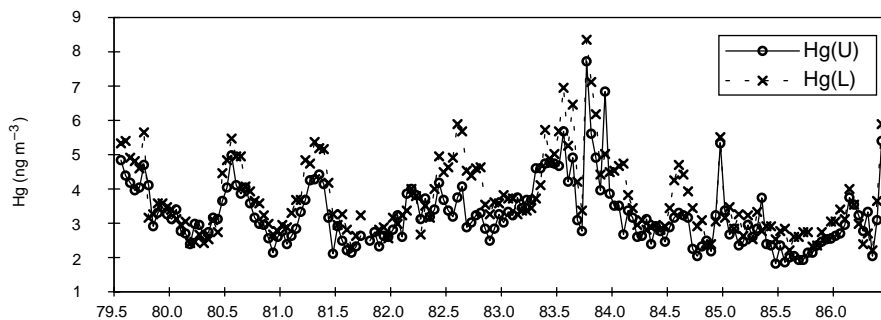
As a simple means to evaluate the strength of the AD, we computed and compared the mean hourly concentrations of PM 10 and PM 2.5. According to this analysis, their mean values were $274 (\pm 233)$ and $132 (\pm 87) \mu\text{g m}^{-3}$, respectively. These concentration levels of PM 10 were about five times higher than the 2-year average of $56.6 \mu\text{g m}^{-3}$ from a southern residential district of Seoul, Korea (Kim and Kim, 2001a). Similarly, the concentrations of CO and O₃ were about 2–3 times higher than those from the urban areas of Korea. We suspect that occasional burning of dry rice paddies near the study site might have caused an increase in CO concentration. However, the presence of unusually high ozone levels (>40 ppb) during this spring season seemed somewhat unusual. On the other hand, the concentrations of oxides (S or N) were comparable to those of the typical background environment, as they are notably lower than those observed in urban areas (or traffic sources).

Employing the stepwise analysis, we attempted to elucidate the mobilization characteristics of Hg under the perturbing environment associated with the AD events. Out of 160 hourly data sets that were assigned with vertical direction, 129 cases showed positive Hg gradient values (i.e., emission from the ground to the atmosphere), while negative ones (dry deposition) were observed for 31 cases. In terms of the Hg concentration at 1 m, the mean value for emission ($3.89 + 1.15 \text{ ng m}^{-3}$) was systematically greater than that for deposition ($3.07 + 0.57 \text{ ng m}^{-3}$). Similarly, for the measured concentration gradients, the former ($0.67 + 0.43 \text{ ng m}^{-3}$) was greater than the latter ($-0.38 + 0.37 \text{ ng m}^{-3}$). Due to unexpected problems associated with the data retrieval, quantification of Hg fluxes was limited to a total of 100 cases. Overall, 83% of the data indicated that the bare rice field was a strong source of Hg with an average emission rate of $229 (+236) \text{ ng m}^{-2} \text{ h}^{-1}$, while significant deposition of PM was accompanied by the intense AD events. The remaining flux data indicated a weak deposition of Hg at nighttime at much lower rate of $-32.3 (+37.5) \text{ ng m}^{-2} \text{ h}^{-1}$.

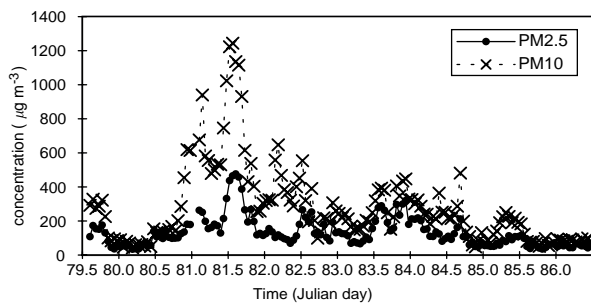
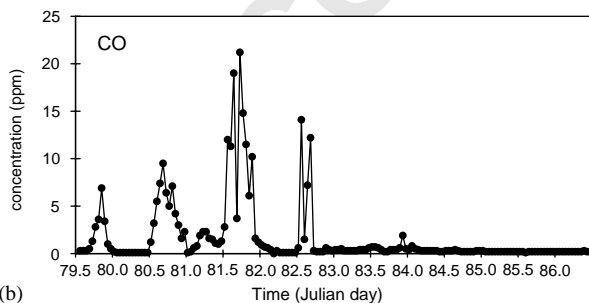
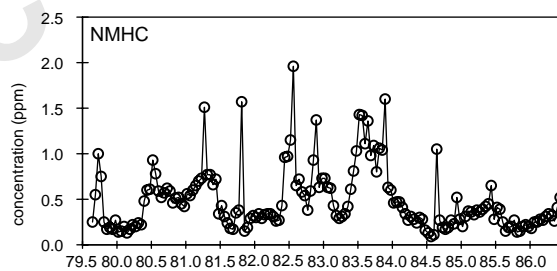
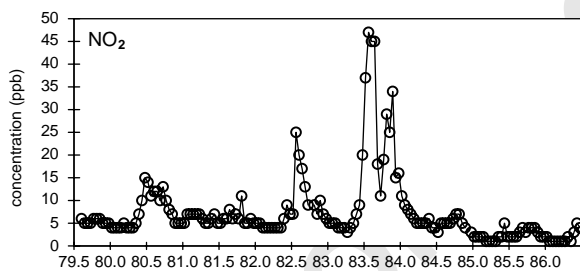
3.2. Temporal variations of Hg concentrations and fluxes

Fig. 3a shows temporal trends of Hg concentrations, gradients, and fluxes during the whole measurement period. The maximum Hg concentration (8.35 ng m^{-3}) occurred at 17:00 on 24 March, while the maximum gradient (2.14 ng m^{-3}) took place earlier at 13:00 on 23 March. The maximum flux of $1071 \text{ ng m}^{-2} \text{ h}^{-1}$ was,

Fig. 3. (a) Plots of temporal variabilities of Hg-related parameters (concentrations, gradients, and fluxes) measured during the whole study period of late March: Julian day 79 corresponds to the 20 March 2001. (b) Plots of temporal variabilities of important pollutant species determined concurrently with Hg measurements. Julian day 79 corresponds to the 20 March 2001.

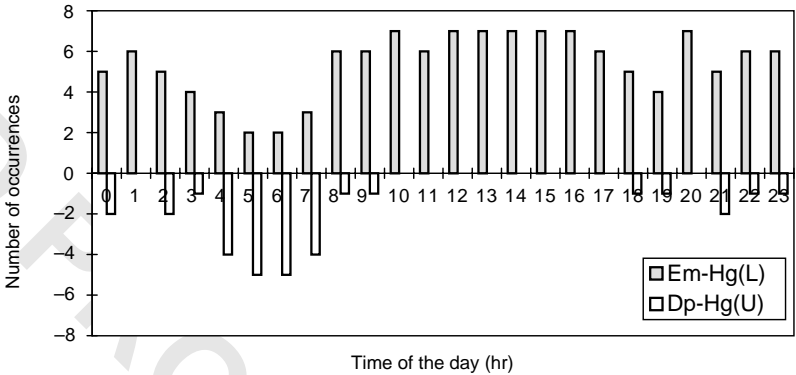
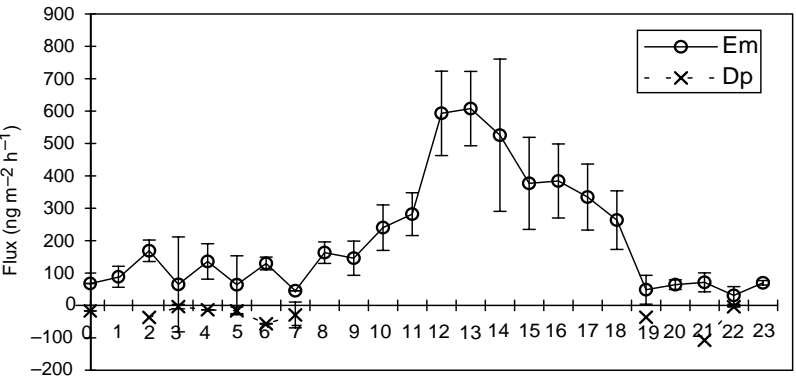
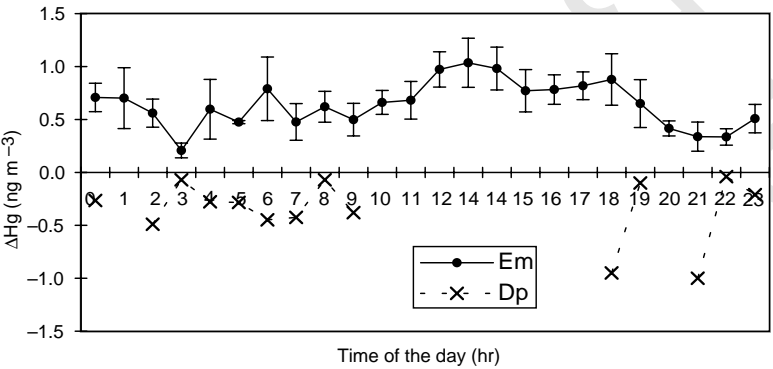
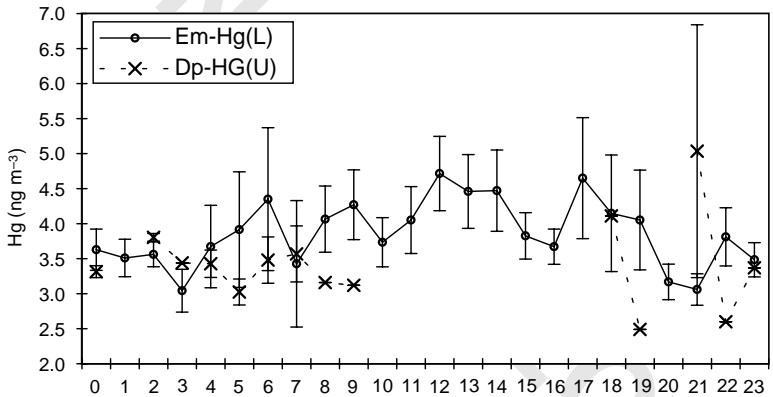


(a)



(b)

1
3
5
7
9
11
13
15
17
19
21
23
25
27
29
31
33
35
37
39
41
43
45
47
49
51
53
55



57
59
61
63
65
67
69
71
73
75
77
79
81
83
85
87
89
91
93
95
97
99
101
103
105
107
109
111

1 however, attained at 14:00 on 25 March. Negative fluxes
 3 (i.e., dry deposition) seemed to occur only during the
 5 certain period of the day. In most cases they occurred
 7 sporadically at nighttime and the maximum concentra-
 9 tion and gradient values were 6.84 and -1.82 ng m^{-3} ,
 11 respectively (21:00 on 24 March). The strongest deposi-
 13 tional flux ($-136 \text{ ng m}^{-2} \text{ h}^{-1}$) was, however, observed at
 15 6:00 on 24 March.

17 The diurnal patterns of Hg are presented in Fig. 4.
 19 Both concentration and flux values were several times
 21 higher during daytime than nighttime. Dry deposition of
 23 Hg occurred at nighttime under stable atmospheric
 25 conditions. The patterns of temporal variations ap-
 27 peared to be highly compatible with the frequency
 29 distribution for emission and dry deposition depicted in
 31 Fig. 4d.

33 Two contrasting patterns of diurnal variability can co-
 35 exist even at the same study site (e.g., Kim and Kim,
 37 2001b; Kviectus et al., 1994). Its patterns are in fact
 39 known to be determined by the two competing mechani-
 41 sms: (1) the strength of source processes which can
 43 accelerate the emission of Hg under certain environ-
 45 mental conditions (such as strong winds or sunlight);
 47 and (2) the meteorological condition leading to the
 49 formation of inversion layer can stimulate the build-up
 51 of Hg above the surface during nighttime (Lee et al.,
 53 1998; Kim and Kim, 2001b). Whereas the former
 55 process is favorable for the daytime enhancement of
 Hg, the latter can lead to opposite direction. Conse-
 quently, the observed diurnal patterns of Hg concentra-
 tion or flux suggest that the influence of the former
 mechanism was dominant at Kang Hwa Island during
 the study period. Although it may be difficult to relate
 diurnal patterns between different compounds, the
 pattern for Hg is not much different from those
 pollutant species investigated concurrently (Fig. 5).

3.3. Comparison of Hg concentrations and fluxes with previous results

When Hg concentration levels are compared between
 present and previous studies, statistically significant
 differences exist. For instance, the results of long-term
 analysis of Hg distribution at two different locations of
 Seoul city (the Han Nam and Yang Jae district)
 indicated that their concentrations were highly compa-
 tible with values exceeding 5 ng m^{-3} , regardless of large
 differences in their land use types (Kim and Kim,
 2001a, b, 2002). Subsequent measurements conducted in
 diverse inland sites of Korea also indicated that their
 concentrations were of similar magnitude (e.g.,

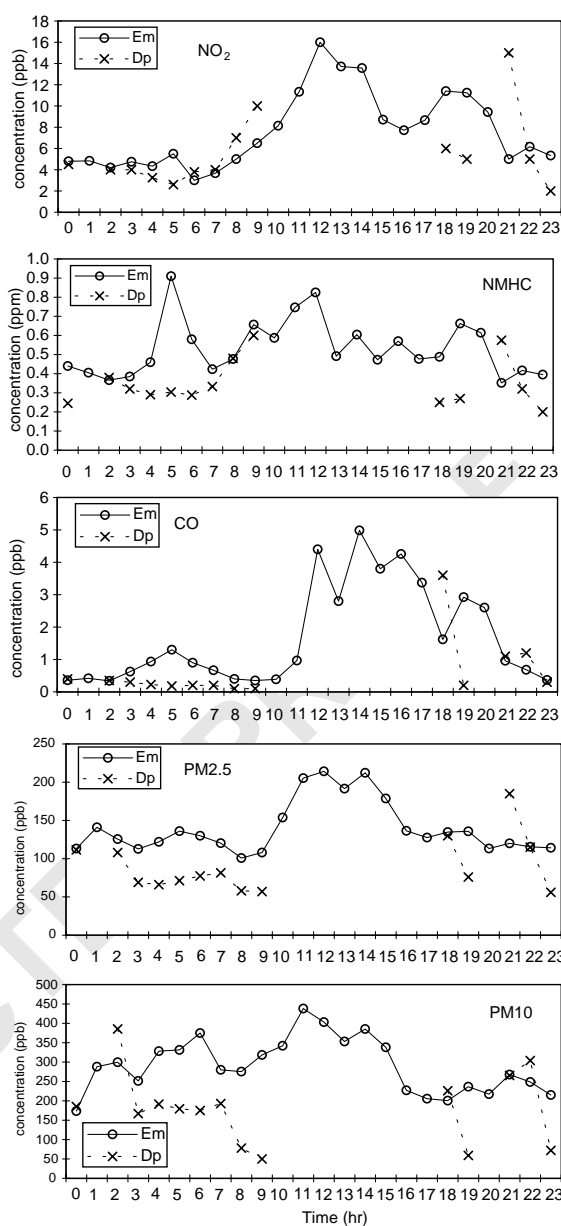


Fig. 5. Diurnal variabilities of important pollutant species determined concurrently with Hg data sets. Symbols Em and Dp denote emission and deposition, respectively.

$> 5 \text{ ng m}^{-3}$ (Kim and Kim, 2001c). Consequently, the
 concentrations of Hg, observable from many urban
 areas of Korea, are clearly distinguished from those of
 relatively remote areas like Kang Hwa Island (e.g.,
 upper 3 ng m^{-3}). The low mean values at Kang Hwa are

Fig. 4. Diurnal variabilities of Hg concentration, gradient, flux, and frequency distribution based on hourly measurement data obtained during the whole study period.

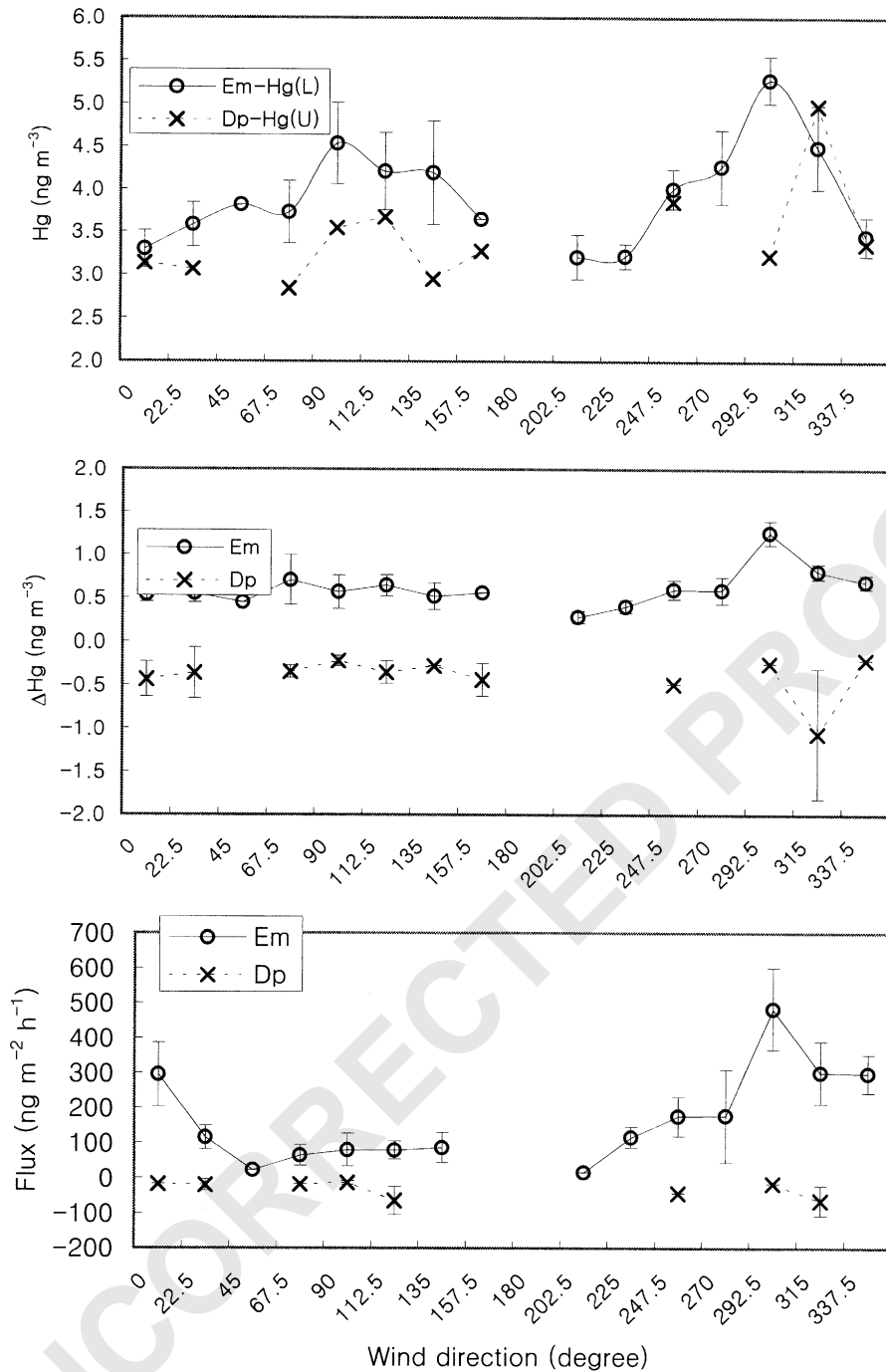


Fig. 6. The plot of Hg data sets (concentration, gradient, and flux) as a function of wind direction.

in fact in compliance with its maximum value (below 10 ng m^{-3}). This result is unique in that excessively high values tend to occur in many of urban locations with its magnitude above a few tens to hundreds of ng (Hg) per cubic meter (Kim and Kim, 2001a, 2002). The Hg

concentration levels at Kang Hwa, are nonetheless still considerably high relative to many background areas of the European or American continents (e.g., $1\text{--}2 \text{ ng m}^{-3}$ levels: Lindberg et al., 1998). Hence, the existence of

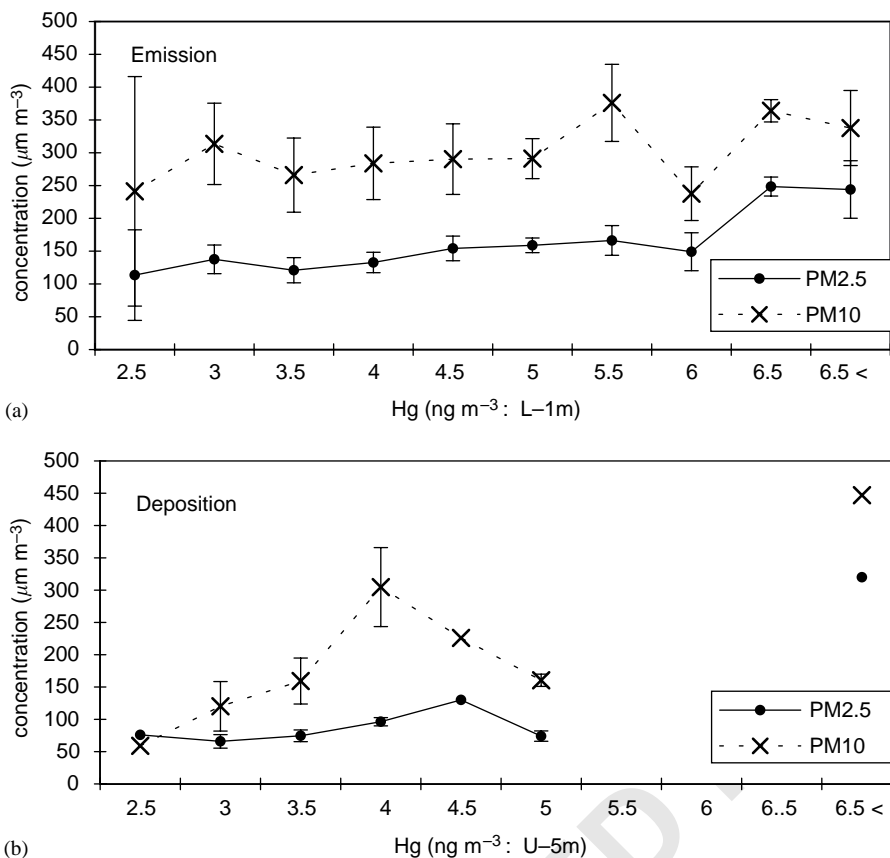


Fig. 7. Relationships between concentration levels of Hg and PM determined during the whole study period. Comparison is made both (1) between emission and deposition and (2) between different PM size.

relatively enhanced Hg levels may be a broad, nationwide phenomenon across the whole Korean peninsula.

The principal features of Hg mobilization at Kang Hwa Island were assessed by quantifying its gradient and flux data. In our study, the Hg emissions were averaged to be $229 + 236 \text{ ng m}^{-2} \text{ h}^{-1}$ ($N = 83$), but the dry deposition was at much reduced value of $-32.3 + 37.5 \text{ ng m}^{-2} \text{ h}^{-1}$ ($N = 17$). Results of previous studies generally indicated that the absolute magnitude of fluxes into two vertical directions tend to be comparable with each other, regardless of large differences in frequency or in source types—whether being clean or polluted. It is, hence, suspected that the deposition flux of smaller magnitude than emission during the present study may have been caused to a certain degree by the perturbed environmental conditions under the influence of AD.

To understand the basic aspects of Hg exchange at the study site, our Hg flux data sets were compared carefully to those reported previously. As a first step, we checked previous results from the background soil environments

including the forest soils of Tennessee, USA (Kim et al., 1995) and clean lake areas of Gardjon, Sweden (Lindberg et al., 1998). These results consistently showed that emission was dominant with the magnitude of around a few $\text{ng m}^{-2} \text{ h}^{-1}$. On the other hand, the previous measurements over contaminated soils such as Hg flooded plain areas in Tennessee (Lindberg et al., 1995) or landfill site in Korea (Kim et al., 2001) showed that the emission fluxes were larger than those of the background area by two to three orders of magnitude. From this respect, the mean emission flux of Kang Hwa of $> 200 \text{ ng m}^{-2} \text{ h}^{-1}$ seems to resemble those observed over contaminated soils.

It may be intriguing to account for what have caused the unusually high fluxes of Hg during our study period. When we focus on the absolute magnitude of Hg concentration gradients, the present results appear to be moderately higher than previous values from clean background areas. To compare the magnitude of concentration gradients among different studies, we used relative gradient value that we obtained by dividing

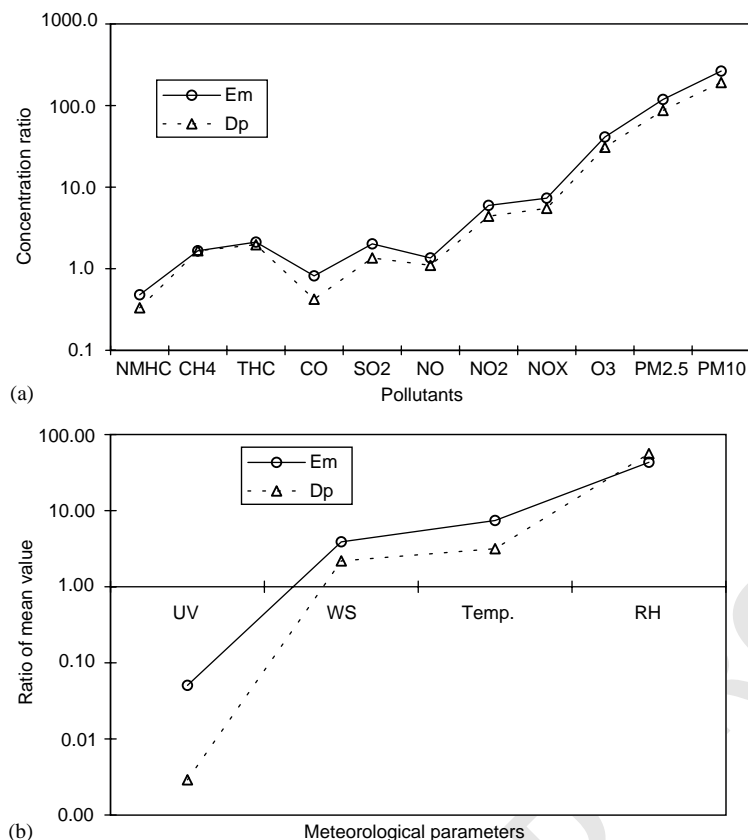


Fig. 8. Comparison of all relevant parameters determined between emission and dry deposition events: (a) pollutants and (b) meteorological parameters. Refer to Table 1 for the actual unit of each parameter.

the absolute gradient value (ng m^{-3}) with the height difference (m) for each gradient study. This was necessary for most measurements adopted different height intervals for their gradient analysis. For emission data sets of the present study, this relative gradient value was $0.168 \text{ ng m}^{-3} \text{ m}^{-1}$. On the other hand, when we use emission data sets for both background forest soil (Kim et al., 1995) and highly contaminated landfill site (Kim et al., 2001), their values ranged from 0.07 to $0.45 \text{ ng m}^{-3} \text{ m}^{-1}$, respectively. The gradient values of the present study are, hence, about two times larger but four times smaller than the two cases. The presence of large Hg fluxes at Kang Hwa, hence, appears to be induced by the prevalence of large turbulent transfer coefficients (K). In this study, K values averaged to be $0.078 \text{ m}^2 \text{ s}^{-1}$ with the range of $0.004\text{--}0.168 \text{ m}^2 \text{ s}^{-1}$. Results of previous studies indicate that the K values determined at the surface environment were generally low. For example, from the analysis made over forest soils in Tennessee, Kim et al. (1995) reported the K values of on average $0.02 + 0.011 \text{ m}^2 \text{ s}^{-1}$. Thus, it may be plausible to say that the substantial enhancement in

emission flux was due largely to strong vertical transfer processes that were more prominent under the influence of the AD event.

3.4. Factors affecting Hg distribution and mobilization at Kang Hwa Island

The results of our Hg study confirmed that its emission strength in the study area was unusually high for a relatively clean environment. The enhanced fluxes resulted largely from highly turbulent conditions during the study period. The possible existence of strong source processes was investigated by examining the flux data as a function of wind direction (Fig. 6). The mean concentrations for the eight wind sectors exhibited both similarity and dissimilarity between emission and deposition data sets. It is seen that the concentration rise was prominent during winds from NW or E, regardless of exchange direction. It is also noted that emission is basically found from all directions, while deposition occurs selectively at certain wind direction. Emission was particularly strong when the prevailing

1
3
5
7
9
11
13
15
17
19
21
23
25
27
29
31
33
35
37
39
41
43
45
47
49
51
53
55

Table 3
Results of correlation analysis between the Hg-related parameters and the relevant environmental parameters measured concurrently during: (a) the upward emission and (b) the downward deposition events

	Hg(U)	ΔHg	Flux	SO ₂	NO	NO ₂	NO _x	CH ₄	NMHC	THC	O ₃	CO	PM2.5	PM10	UV	RH	WS	Temp.	
<i>(A) Emission data sets</i>																			
Hg(L)	<i>r</i> [*]	0.930 ^{III}	0.576 ^{III}	0.375 ^{II}	0.502 ^{III}	0.467 ^{III}	0.629 ^{III}	0.615 ^{III}	0.345 ^{III}	0.607 ^{III}	0.658 ^{III}	0.243 ^I	-0.042	0.234 ^I	0.036	0.225	0.141	-0.291 ^{II}	0.394 ^{III}
	<i>P</i>	3.3E-19	6.6E-13	4.8E-04	1.8E-09	3.1E-08	5.4E-16	4.6E-15	7.2E-05	1.6E-14	2.2E-18	5.5E-03	6.4E-01	8.4E-03	6.9E-01	1.0E-02	1.1E-01	8.3E-04	3.8E-06
Hg(U)	<i>r</i>	0.235 ^I	0.094	0.460 ^{III}	0.400 ^{III}	0.549 ^{III}	0.535 ^{III}	0.234	0.541 ^{III}	0.572 ^{III}	0.219	-0.073	0.140	-0.006	0.115	0.217	-0.316 ^{II}	0.319 ^{II}	
	<i>P</i>	7.3E-03	4.0E-01	5.5E-08	3.3E-06	2.1E-11	8.3E-11	8.0E-03	4.6E-11	1.5E-12	1.3E-02	4.1E-01	1.2E-01	9.4E-01	1.9E-01	1.3E-02	2.7E-04	2.2E-04	
ΔHg	<i>r</i>		0.755 ^{III}	0.306 ^{II}	0.350 ^{III}	0.447 ^{III}	0.442 ^{III}	0.389 ^{III}	0.402 ^{III}	0.468 ^{III}	0.156	0.053	0.307 ^{II}	0.108	0.339 ^{III}	-0.110	-0.067	0.332 ^{II}	
	<i>P</i>		2.7E-18	4.6E-04	5.4E-05	1.4E-07	2.0E-07	6.3E-06	2.8E-06	3.0E-08	7.7E-02	5.5E-01	4.7E-04	2.3E-01	8.3E-05	2.1E-01	4.5E-01	1.2E-04	
Flux	<i>r</i>			0.285 ^I	0.476 ^{III}	0.390 ^{II}	0.428 ^{III}	0.456 ^{III}	0.243	0.339 ^I	0.103	0.159	0.191	0.010	0.645 ^{III}	-0.374 ^{II}	0.158	0.425 ^{III}	
	<i>P</i>			9.0E-03	6.2E-06	3.0E-04	6.2E-05	1.5E-05	2.7E-02	1.7E-03	3.6E-01	1.5E-01	8.8E-02	9.3E-01	2.7E-11	4.9E-04	1.5E-01	6.1E-05	
<i>(B) Deposition data sets</i>																			
Hg(L)	<i>r</i>	0.923 ^{III}	-0.512 ^I	-0.568	0.388	-0.076	0.513 ^I	0.488 ^I	0.162	0.416	0.490 ^I	0.099	0.317	0.606 ^{II}	0.482 ^I	-0.104	0.103	-0.022	0.205
	<i>P</i>	1.1E-10	3.2E-03	1.7E-02	3.1E-02	6.9E-01	3.7E-03	6.3E-03	3.8E-01	2.0E-02	5.1E-03	6.0E-01	8.2E-02	3.0E-04	6.0E-03	5.8E-01	5.8E-01	9.1E-01	2.7E-01
Hg(U)	<i>r</i>		-0.803 ^{III}	-0.719 ^I	0.554 ^I	0.033	0.588 ^{II}	0.577 ^{II}	0.254	0.471 ^I	0.557 ^I	0.290	0.457 ^I	0.728 ^{III}	0.439	-0.092	-0.016	-0.041	0.301
	<i>P</i>		5.4E-08	1.1E-03	1.2E-03	8.6E-01	6.3E-04	8.5E-04	1.7E-01	7.5E-03	1.1E-03	1.1E-01	9.7E-03	3.5E-06	1.3E-02	6.2E-01	9.3E-01	8.2E-01	1.0E-01
ΔHg	<i>r</i>			0.825 ^{III}	-0.637 ^{II}	-0.192	-0.520 ^I	-0.534 ^I	-0.316	-0.408	-0.484 ^I	-0.495 ^I	-0.530 ^I	-0.687 ^{III}	-0.234	0.044	0.196	0.058	-0.355
	<i>P</i>			4.6E-05	1.2E-04	3.1E-01	3.2E-03	2.4E-03	8.3E-02	2.3E-02	5.8E-03	4.7E-03	2.2E-03	2.0E-05	2.1E-01	8.2E-01	2.9E-01	7.6E-01	5.0E-02
Flux	<i>r</i>				-0.470	-0.028	-0.514	-0.513	-0.149	-0.569	-0.511	-0.321	-0.390	-0.391	0.064		0.074	0.015	-0.387
	<i>P</i>				5.7E-02	9.1E-01	3.5E-02	3.5E-02	5.7E-01	1.7E-02	3.6E-02	2.1E-01	1.2E-01	1.2E-01	8.1E-01		7.8E-01	9.5E-01	1.3E-01

**r* and *P* denote correlation coefficients and probability of no correlation, respectively.
Superscripts I, II, and III denote *P* values < 10⁻², 10⁻³, and 10⁻⁴, respectively.

57
59
61
63
65
67
69
71
73
75
77
79
81
83
85
87
89
91
93
95
97
99
101
103
105
107
109
111

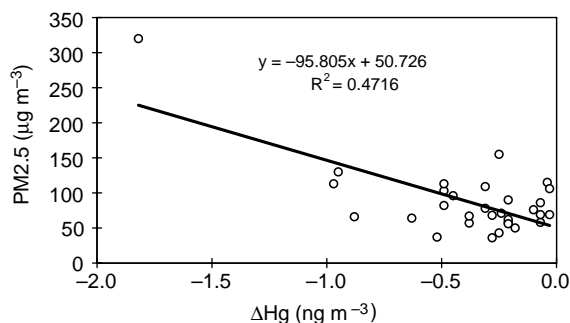


Fig. 9. Relationships between PM 2.5 and the concentration gradient of Hg during deposition events.

wind was from NW to N, suggesting heterogeneous distribution of Hg sources at the study site. The patterns found from this analysis during deposition are in agreement with the general expectation. It can be inferred that the Hg concentration in the study area be affected either by long-range transport (e.g., the mainland China (NW)) or by local inland sources (such as Seoul city on E-SE).

In light of the unusual environmental conditions of the study period during which excessive amount of aerosols were transported, it may be desirable to investigate the Hg behavior in its relationship with PMs. If the overall temporal variability was compared between Hg and PM (Fig. 3), some similarities can be seen. To check for the possible relationships between them, we made a direct comparison of their concentration levels after sorting them into a number of classes. The results of this comparison, shown in Fig. 7, indicate that the patterns are highly contrasting between emission and dry deposition; almost no deposition occurred above the Hg concentration of 5 ng m^{-3} , while emission was observed indiscriminately at all concentration range. During the emission events, the concentration of Hg tended to increase slightly with increasing PM concentration. In addition, changes of PM values against Hg concentration levels appeared to be much stable during emission than deposition events.

In order to study the possible effects of environmental conditions that are potent enough to determine or influence the vertical exchange of Hg, we compared the mean values of all the concurrently determined environmental parameters after dividing them in accordance with the vertical directions of Hg exchange. When the means for each parameter between two directions were compared, the values for emission were systematically larger than its counterpart (Fig. 8a and b). Such differences in concentration levels were most distinctive for both PM 2.5 and PM 10. In case of meteorological parameters, the patterns were quite contrasting between RH and all others investigated (Fig. 8b). While emission

appeared to be favored under low humidity, it was not the case for other parameters. For temperature and wind speed, emission seemed to be advantageous with their increase; but such distinction was weak for UV. The effect of temperature or wind speed on Hg mobilization, especially on the activation of upward emission has been reported previously (Kim et al., 1995; Kim and Kim, 1999).

To further study the relationships between Hg and other environmental parameters, we conducted correlation analysis separately for each of the two vertical directions (Table 3). The number of strongly correlated pairs was substantially larger for upward emission than for downward deposition. In case of emission, the Hg concentrations at lower level (1 m) tended to exhibit both positive and inverse correlations (of high statistical significance) with temperature and wind speed, respectively. Relationships between Hg flux and meteorological parameters were, however, different as its upward flux seemed to be strongly correlated with temperature (or irradiance) instead of wind speed. It is, hence, possible to conclude that temperature could maintain strong relationships with both its concentration and flux, while wind speed may be rather complicated. The significance of temperature as the controlling mechanism of Hg emission has been documented previously (e.g., Lindberg et al., 1995).

Relationships between Hg and other trace gases seem to exhibit a number of interesting facets of Hg geochemistry. Most importantly, the concentration of Hg during emission showed the most abundant and strongest correlations with all pollutants (except for a few cases including CO and PM 10). This observation thus suggests that the basic factors determining air quality can also be influential on Hg emission. For reference in our comparative studies of Hg distributions in Seoul city between the present (the late 90s) and the past (the late 80s), the results for the former period appeared to be affected more sensitively by the factors regulating the general air quality than the latter (Kim and Kim, 2002). By contrast, in the case of dry deposition, the pattern is seen to be highly different. (In this case, the concentration of Hg at upper height of 5 m was used to compare its relationship with others.) It is seen that the concentration of Hg alone could maintain relatively strong correlations with several pollutants including PM 2.5. In fact, examinations of relationships between Hg and PM were attempted previously from the measurements made in the Amazon basin (Artaxo et al., 2000). Although intended for assessing large-scale distribution characteristics of Hg, their studies revealed many interesting aspects on the relationships between Hg and PM. They conducted concurrent measurements of total gaseous Hg, PM, and PM-bound metals during the peak of biomass burning season, when large amount of Hg was believed to be

released. They concluded that about 31% of Hg was associated with the biomass burning, while the dominant portion of Hg was accounted for by the exceedingly high mining activities. To account for strong relationships between Hg and biomass burning particles, they proposed three different mechanisms: (1) adsorption of gaseous Hg on existing particles; (2) direct release of Hg from biomass burning; and (3) evaporation of Hg from soil as the result of forest burning.

The burning of dry rice paddies, observed occasionally during our study period, may have similar implications to the above-mentioned biomass burning. While such occurrences can lead to the deterioration of the general air quality, its impact might have been reflected most critically in pollutants such as CO and PM. In case of PM, the results of the correlation analysis showed that Hg maintained strong correlations with fine rather than coarse fraction of PM. It is interesting to note that the results for CO and PM 2.5 were highly contrasting between emission and deposition (Table 3). In general, the strength and abundance of significantly correlated pairs were reduced noticeably during deposition relative to emission. However, the results for CO and PM 2.5 are much different from others because they showed more enhancements for deposition data sets. This result thus suggests that under our measurement conditions those pollutants behaved as incisive indicators for the downward deposition of Hg. Moreover, it is striking to note that the concentration of PM 2.5 exhibited both positive and inverse correlations with Hg concentration gradient, while such relations appeared to be much significant during downward deposition. Although the relationships depicted in Fig. 9 can be erroneous due to the dominance of trend by one large data point, it still leaves the possibility that the deposition of Hg can be affected by the increasing loading of fine particles. The formation of particles via burning processes can release large quantities of black carbon with high potential to absorb gaseous Hg. However, the existence of opposite trend in which PM 2.5 tended to increase with Hg gradients observed during emission events can also be accountable, if one considers that the burning process could release Hg via two mechanisms suggested by Artaxo et al. (2000).

4. Conclusions

The distribution and exchange characteristics of total gaseous Hg were investigated from a relatively clean soil environment of Kang Hwa Island, Korea. Results of our study indicate that the mean concentration of upper 3 ng m^{-3} is relatively lower than those of other Korean environments but significantly larger than those of background soils in Europe or America. When the exchange patterns of Hg were examined, distinctive

differences were apparent between emission and deposition from various respects. Comparison of the frequency distribution patterns indicates that emission outnumbered deposition by about four times. Moreover, the strength of emission was large with $220 \text{ ng m}^{-2} \text{ h}^{-1}$, while that for deposition was estimated at much reduced value of $-32 \text{ ng m}^{-2} \text{ h}^{-1}$. Such levels of emission flux are more compatible with those measured previously from highly contaminated areas rather than those of relatively clean soil environments. The results thus indicate moderately high-concentration level of Hg but unusually high fluxes for a relatively unpolluted environment.

During the course of our field study, we were able to examine the bi-directional exchange characteristics of Hg under complicated environmental conditions. The environmental conditions of Hg mobilization were examined more specifically for both emission and deposition. The emission of Hg appeared to be associated with the increasing concentration levels of other pollutants, typically accompanied by high temperature and low humidity. On the other hand, dry deposition of Hg was favored with high loadings of fine particles or CO. When the patterns of bi-directional exchange were further investigated by the correlation analysis, the results were clearly distinguished between pollutants and meteorological parameters. Unlike the cases of meteorological parameters, significantly correlated cases were highly abundant between Hg and pollutants, especially for emission data sets. It was, however, found that the concentration change of some pollutants including CH_4 might be more sensitively reflected on the upward flux of Hg, while most pollutants basically seemed to maintain strong correlations with Hg. In addition, it should be pointed out that the pattern for dry deposition was much different from that of emission. The strong association between Hg gradient and fine particle levels suggests that the extent of Hg exchange, whether being upward emission or downward deposition, can be affected by and large through different mechanisms by the transport and/or formation of particles.

5. Uncited reference

Kvietkus and Sakalys, 1998.

Acknowledgements

This research was supported by the Climate Environmental System Research Center sponsored by the Korean Science and Engineering Foundation (KOSEF). The third author would also like to thank for a support from the Brain Korea 21 Project.

1 **References**

- 3 Artaxo, P., de Campos, R.C., Fernandes, E.T., Martins, J.V.,
5 Xiao, Z., Lindqvist, O., Fernandez-Jimenez, M.T., Maen-
7 haut, W., 2000. Large scale mercury and trace element
9 measurements in the Amazon basin. *Atmospheric Environ-*
11 *ment* 34, 4085–4096.
- 13 Edwards, G.C., Rasmussen, P.E., Schroeder, W.H., Kemp,
15 R.J., Dias, G.M., Fitzgerald-Hubble, C.R., Wong, E.K.,
17 Halfpenny-Mitchell, L., Gustin, M.S., 2001. Sources of
19 variability in mercury flux measurements. *Journal of*
21 *Geophysical Research* 106, 5421–5435.
- 23 Kaimal, J.C., Finnigan, J.J., 1994. *Atmospheric Boundary*
25 *Layer Flows: Their Structure and Measurement*. Oxford
27 University Press, Oxford, 289pp.
- 29 Kim, K.-H., Kim, M.-Y., 1999. The exchange of gaseous
31 mercury across soil–air interface in a residential area of
33 Seoul, Korea. *Atmospheric Environment* 33, 3153–3165.
- 35 Kim, K.-H., Kim, M.-Y., 2001a. The temporal distribution
37 characteristics of total gaseous mercury at an urban
39 monitoring site in Seoul during 1999–2000. *Atmospheric*
41 *Environment* 35, 4253–4263.
- 43 Kim, K.-H., Kim, M.-Y., 2001b. Some insights into short-term
45 variability of total gaseous mercury in urban air. *Atmo-*
47 *spheric Environment* 35, 49–59.
- 49 Kim, M.-Y., Kim, K.-H., 2001c. Regional distribution char-
51 acteristics of total gaseous mercury in air-measurements
53 from urban and mountainous sites in Korea. *Journal of*
55 *Korean Society for Atmospheric Environment* 17, 39–50.
- 57 Kim, K.-H., Kim, M.-Y., 2002. A decadal shift in total gaseous
59 mercury concentration levels in Seoul, Korea: changes
61 between the late 80s and late 90s. *Atmospheric Environ-*
63 *ment* 36, 663–675.
- 65 Kim, K.-H., Lindberg, S.E., 1994. High-precision measure-
67 ments of mercury vapor in air: design of a six-port-manifold
69 mass flow controller system and evaluation of mass flow
71 errors at atmospheric pressure. *Journal of Geophysical*
73 *Research* 99, 5379–5384.
- 75 Kim, K.-H., Lindberg, S.E., Meyers, T.P., 1995. Micrometeor-
77 ological measurements of mercury vapor fluxes over back-
ground forest soils in eastern Tennessee. *Atmospheric*
Environment 29, 267–282.
- Kim, K.-H., Paul, J.H., Barnett, M., Lindberg, S.E., 1997. Biogeochemistry of mercury in the air–soil–plant system. In: Siegel H. (Ed.), *Metal Ions in Biological Systems*, Vol. 34. Marcel Dekker, New York, pp. 185–212 (Chapter 7).
- Kim, K.-H., Kim, M.Y., Lee, G., 2001. The soil–air exchange characteristics of total gaseous mercury from a large scale municipal landfill area. *Atmospheric Environment* 35, 3475–3493.
- Kvietkus, K., Sakalys, J., 1998. Diurnal variations in mercury concentrations in the ground layer atmosphere. In: Watras, C.J., Huckabee, J.W. (Eds.), *Mercury Pollution: Integration and Synthesis*. Lewis Publishers, Boca Raton, FL, USA, pp. 243–250.
- Lee, D.S., Dollard, G.J., Pepler, S., 1998. Gas-phase mercury in the atmosphere of the United Kingdom. *Atmospheric Environment* 32, 855–864.
- Lee, X., Benoit, G., Hu, X., 2000. Total gaseous mercury concentration and fluxes over a coastal saltmarsh vegetation in Connecticut, USA. *Atmospheric Environment* 34, 4205–4213.
- Lin, C., Penkonen, S.O., 1999. The chemistry of atmospheric mercury: a review. *Atmospheric Environment* 33, 2067–2079.
- Lindberg, S.E., Kim, K.-H., Meyers, T.P., Owens, J.G., 1995. Micrometeorological gradient approach for quantifying air/surface exchange of mercury vapor: tests over contaminated soils. *Environmental Science and Technology* 29 (1), 126–135.
- Lindberg, S.E., Hanson, P.J., Meyers, T.P., Kim, K.-H., 1998. Air/surface exchange of mercury vapor over forests: the need for a reassessment of continental biogenic emissions. *Atmospheric Environment* 32, 895–908.
- Meyers, T.P., Hall, M., Lindberg, S.E., Kim, K.-H., 1996. Use of the MBR technique to measure fluxes of trace species. *Atmospheric Environment* 30 (19), 3321–3329.
- Perry, K.D., Cahill, T.A., Schnell, R.C., Harris, J.M., 1999. Long-range transport of anthropogenic aerosols to the National Oceanic and Atmospheric Administration baseline station at Mauna Loa Observatory, Hawaii. *Journal of Geophysical Research* 104, 18521–18533.
- Wallschlager, D., Kock, H.H., Schroeder, W.H., Lindberg, S.E., Ebinghaus, R., Wilken, R.D., 2000. Mechanism and significance of mercury volatilization from contaminated flood-plains of the German river Elbe. *Atmospheric Environment* 34, 3745–3755.